

# The Continuum Percolation Threshold for Interpenetrating Squares and Cubes

Don R. Baker,<sup>\*†</sup> Gerald Paul,<sup>\*</sup> Sameet Sreenivasan,<sup>\*</sup> and H. Eugene Stanley<sup>\*</sup>

<sup>\*</sup>*Center for Polymer Studies and Dept. of Physics, Boston University, Boston, MA 02215 USA*

<sup>†</sup>*Department of Earth and Planetary Sciences, McGill University*

*3450 rue University, Montréal, QC H3A 2A7 Canada*

(11 March 2002)

Monte Carlo simulations are performed to determine the critical percolation threshold for interpenetrating square objects in two dimensions and cubic objects in three dimensions. Simulations are performed for two cases: (i) objects whose edges are aligned parallel to one another and (ii) randomly oriented objects. For squares whose edges are aligned, the critical area fraction at the percolation threshold  $\phi_c = 0.6666 \pm 0.0004$ , while for randomly oriented squares  $\phi_c = 0.6254 \pm 0.0002$ , 6% smaller. For cubes whose edges are aligned, the critical volume fraction at the percolation threshold  $\phi_c = 0.2773 \pm 0.0002$ , while for randomly oriented cubes  $\phi_c = 0.2236 \pm 0.0002$ , 24% smaller.

## I. INTRODUCTION

Lattice percolation is often used for the statistical modeling of transport in porous media [1–4]. The requirement that sites, and the bonds between them, be constrained to a fixed lattice may not, however, be an appropriate model for natural porous media [1–4]. The characteristics of site and bond percolation potentially limit their applicability to modeling of natural phenomena such as oil or groundwater flow and extraction of melt from super-solidus regions deep inside a planetary body.

Continuum percolation offers two advantages for describing porous media:

- (i) The objects which form clusters are not restricted to points on a fixed lattice; they can be placed anywhere within the volume studied and either be barred from interpenetration, or allowed to interpenetrate, i.e., they can have either “hard” or “soft” cores [4]. Because of the freedom of placement inside the system, the connections between soft core objects can range from very small to very large, depending upon the extent of interpenetration.
- (ii) The objects can be of any shape. In two dimensions the continuum percolation of discs is often investigated [2,4]. In most studies of continuum percolation in three dimensions, spheres are used as the objects, leading to the “swiss-cheese” nomenclature for continuum percolation [2,4]. Other frequently-used shapes are rods and ellipsoids of revolution [5]. In a few cases the continuum percolation of cubes has been considered [6].

Here we determine the threshold for continuum percolation of soft core squares in two dimensions (2-D) and cubes in three dimensions (3-D) whose edges are aligned parallel to, or oriented at random angles to, the axes of the system. Continuum percolation is believed to belong to the same universality class as site and bond percolation

[7,8]; once we have determined the continuum threshold for an object of a specific shape we can apply many of the characteristics of site and bond percolation, e.g. critical exponents, to describe the continuum percolation cluster.

## II. METHODS

We construct 2-D and 3-D Monte Carlo simulations for the determination of the percolation threshold based upon the Leath method [9] and the methods Lorenz and Ziff [10] used in their study of the continuum percolation of spheres.

We perform 2-D simulations with squares whose edges are of unit length. In 3-D we perform simulations with cubes of three different edge lengths:  $1/\sqrt{3}$ , 0.75, and 1.0; the length  $L$  of each axis of the simulation box in the 2-D simulations is 301, and in 3-D is 101 in simulations using cubes with edge lengths of  $1/\sqrt{3}$  and 0.75, and is 161 in simulations with the unit cube [11]. We subdivide the system into either a 2-D or 3-D grid of unit area squares or unit volume cubes; an illustrative  $12 \times 12$  2-D version of our system is shown in Fig. 1.

The cluster begins in the center grid volume and objects are added to it based upon a Poisson distribution centered about the average number of objects per unit area or volume,  $N/L^d$ , chosen for the simulation of dimension  $d$  [10]. The product of this value and the individual object’s area or volume,  $v$ , is the reduced number density

$$\eta \equiv \frac{vN}{L^d}. \quad (1)$$

If the number of objects,  $n$ , generated from the Poisson distribution is nonzero, then these  $n$  objects are placed at random locations inside the grid volume. To fix the orientation of each individual object, random numbers are generated to determine the one angle of rotation in the 2-D simulations and the three Euler angles of rotation in the 3-D simulations; these angles vary between

0 and  $2\pi$ . The locations of the 4 (2-D) or 8 (3-D) corners and the center of each object are stored in a data structure, along with a flag indicating that the grid area (2-D) or volume (3-D) was visited and populated during the realization. The nearest-neighbors and next-nearest-neighbors of this grid area or volume are then populated in a similar manner and the intersection between squares or cubes is tested.

To determine whether two squares intersect we choose one square in the cluster as the reference square and another square in the simulation as the test square. We use an algorithm for the intersection of two lines [12] to test if any of the 4 edges of the reference square intersect the 4 edges of the test square. To determine if two cubes intersect we choose one cube in the cluster as the reference cube and another in the simulation as the test cube. We use an algorithm for the intersection of a line and a facet [13] to test if any of the edges of the reference cube intersect the faces of the test cube. In this algorithm, the location of each of the 12 edges of the reference cube are compared to the location of the 12 triangular facets that describe the locations of all faces on the test cube using the corners and diagonal of each face. If the test object intersects the reference object, it is added to the growing cluster. This process is repeated for each new square or cube added to the system until the cluster can no longer grow. Intersections between squares or cubes in grid areas or volumes up to two units away can occur for edge lengths 0.75 and 1, as exemplified in 2-D for squares of unit edge (Fig. 1), but cubes of edge  $1/\sqrt{3}$  can only intersect if they are in the same or neighboring volumes of the grid, which reduces the number of grid volumes that must be checked for cube overlap in simulations with cubes of this smallest size.

The cumulative distribution of cluster sizes is calculated from the cluster size of each realization,  $s$ , by binning the cluster sizes such that all bins in the range of  $2^0$  to  $2^{s+1} - 1$  are incremented by 1. In order to estimate finite-size effects of the simulation, objects in each cluster are tested to determine whether they touch the edge of the simulation. If so, the cluster size is compared against the smallest cluster size in previous realizations that touch the edge and the smaller value is stored. Bins of size greater than the smallest cluster that touched the edge of the system are not used in the determination of the percolation threshold.

At the end of the simulation, the value of each bin is divided by the number of realizations, from 10,000 to 50,000, to yield the probability of achieving a cluster of size  $s$ ,  $P(s|\eta)$ , for a given value of  $\eta$ . Power law behavior of the probability as a function of the bin size is interpreted to indicate the critical percolation threshold  $\eta = \eta_c$  [2,4]. To accurately determine the threshold, we follow the techniques of Ref. [10]. The probability of generating a cluster size  $s$  at a specified  $\eta$  is [2,4]

$$P(s|\eta) \sim As^{2-\tau}f[(\eta - \eta_c)s^\sigma], \quad (2)$$

where both  $\tau$  and  $\sigma$  are universal exponents and  $A$  is

a non-universal constant. In 2-D the values of these exponents are 187/91 and 36/91 [4], respectively. In 3-D the values of  $\tau$  and  $\sigma$  are  $2.18906 \pm 0.00006$  and  $0.4522 \pm 0.0008$ , respectively [14]. Near the percolation threshold the scaling function  $f(x)$  can be expanded in a Taylor series

$$f(x) = 1 + Bx + \mathcal{O}(x^2). \quad (3)$$

Combining Eqs. (2) and (3),

$$P(s|\eta)s^{\tau-2} \sim A + AB(\eta - \eta_c)s^\sigma + \dots \quad (4)$$

which demonstrates that  $P(s|\eta)s^{\tau-2}$  becomes constant at the percolation threshold as  $s$  becomes asymptotically large.

### III. RESULTS

The percolation threshold can be expressed either as the critical reduced number density,  $\eta_c$ , or the critical area (or volume) fraction,  $\phi_c$ , which are related to each other by [15]

$$\phi_c = 1 - e^{-\eta_c}. \quad (5)$$

#### A. Two Dimensions

For square objects aligned parallel to each other in the 2-D system we find

$$\eta_c = 1.098 \pm 0.001 \quad (6a)$$

or, from (5),

$$\phi_c = 0.6666 \pm 0.0004 \quad (6b)$$

(see Fig. 2a). Our value of  $\phi_c$  is within the error bars of two previous determinations by Monte Carlo techniques, where  $\phi_c = 0.668 \pm 0.003$  [16] and  $\phi_c = 0.65 \pm 0.02$  [17]. However our determination of  $\phi_c$  is slightly lower than that calculated by [6] whose Monte Carlo simulations produced  $\phi_c = 0.6753 \pm 0.0008$ , and whose application of the direct-connectedness expansion method yielded  $\phi_c = 0.6912$ . In contrast, our value of  $\phi_c$  is significantly higher than the experimental one of [18] whose average for 9 trials is  $\phi_c = 0.613 \pm 0.013$ .

We find that for randomly oriented square objects in 2-D

$$\eta_c = 0.9819 \pm 0.0006 \quad (7a)$$

or

$$\phi_c = 0.6254 \pm 0.0002 \quad (7b)$$

(see Fig. 2b). This is the first determination of these values for randomly oriented squares.

These values for the continuum percolation threshold for aligned and randomly oriented squares are lower than for discs,  $\phi_c = 0.67$  [19], by a maximum of  $\approx 0.5\%$  for aligned squares and  $\approx 7\%$  for randomly oriented squares. We attribute the significant difference in  $\phi_c$  between discs and randomly oriented squares to the possibility of randomly oriented squares intersecting other squares whose centers are located at distances up to the diagonal length of the square (see Fig. 1), whereas two discs can only intersect if their centers are no further than one diameter away from each other. The similarity of  $\phi_c$  for aligned squares and discs may occur because both objects can only possibly intersect other objects whose centers are separated at most by either the edge length of the square or the diameter of the disc.

## B. Three Dimensions

For cubic objects aligned parallel to each other in the 3-D system,

$$\eta_c = 0.3248 \pm 0.0003 \quad (8a)$$

or

$$\phi_c = 0.2773 \pm 0.0002 \quad (8b)$$

(see Fig. 3a). The precision of this result is greater than the most precise previous determination  $\phi_c = 0.280 \pm 0.005$  [6]. The critical volume fraction is significantly less when cubic objects are allowed to have random orientations,

$$\eta_c = 0.2531 \pm 0.0003 \quad (9a)$$

or

$$\phi_c = 0.2236 \pm 0.0002 \quad (9b)$$

(see Fig. 3b). The result for randomly oriented cubes is the same for cubes of edge-length  $1/\sqrt{3}$ , 0.75, and 1. Thus, as expected, the percolation threshold is independent of the cube and system size used. This value is the first determination of  $\phi_c$  for the continuum percolation of randomly oriented cubes.

Comparision of the critical volume at the percolation threshold for aligned cubes with that determined for spheres,  $\phi_c = 0.289573 \pm 0.000002$  [10], demonstrates that the difference in shape between spheres and cubes affects  $\phi_c$  by  $\approx 4\%$  [6]. Allowing cubes to randomly orient lowers  $\phi_c \approx 23\%$ . The difference between the randomly oriented cubes and spheres is due to the same process as discussed above for discs and squares, but in this case it is the greater length of the body diagonals of cubes compared to the diameter of spheres or the edge length of aligned cubes that enhances the probability of connectedness for randomly oriented cubes at any given volume fraction.

## IV. DISCUSSION

The continuum percolation threshold can be predicted with excluded volume theory [6,20,22]:

$$N_c V_{\text{ex}} = B_c, \quad (10)$$

where  $N_c$  is the critical density of objects [23],  $V_{\text{ex}}$  is their excluded area or volume, and  $B_c$  is the average number of bonds per object [21]. Originally,  $B_c$  was thought to be one constant for all parallel (i.e., not randomly oriented) convex objects in 2-D and another constant in 3-D [21], but later  $B_c$  was determined to be different for spheres and for cubes in 3-D [6]. The excluded area for discs and aligned squares of unit area is 4 and for randomly oriented unit squares 4.084 [20]. For both spheres and aligned cubes  $V_{\text{ex}}$  is equal to 8 times their volume in 3-D. For randomly oriented cubes  $V_{\text{ex}}$  is 11 times their volume [24]. Calculated values of  $B_c$  in 2-D and 3-D are presented in Table I.

In 2-D we determine  $B_c = 4.39 \pm 0.01$  for aligned squares and for randomly oriented squares  $B_c = 4.01 \pm 0.01$ . The value for aligned squares is similar to that originally proposed by Balberg for discs and squares,  $B_c = 4.5 \pm 0.1$  [21] and to the values for discs and squares calculated from Monte Carlo simulations:  $B_c = 4.43$  [19] and  $B_c = 4.5 \pm 0.1$  [6], respectively. On the other hand our value for  $B_c$  is somewhat lower than calculated by a series expansion technique,  $B_c = 4.7$  [6]. Thus we confirm that  $B_c$  has the same value, within error, for discs and for aligned squares in 2-D. However, a different behavior is observed when squares are randomly oriented and  $B_c$  drops by  $\approx 10\%$ , consistent with expectations that non-parallel objects should exhibit a lower  $B_c$  than parallel objects [20].

Our Monte Carlo simulations yield  $B_c = 2.59 \pm 0.01$  for aligned cubes, as is expected because of the agreement between our estimate of the percolation threshold and previous estimates. For randomly oriented cubes  $B_c = 2.78 \pm 0.01$ , within error of  $B_c$  for the continuum percolation of spheres [6]. This result is surprising in light of the observation that  $B_c$  for randomly oriented squares is  $\approx 10\%$  below aligned squares and is contrary to expectations that randomly oriented objects should have lower values of  $B_c$  than aligned ones [20]. However,  $B_c$  for randomly oriented cubes does not exceed the limiting value predicted by the excluded volume theory of the continuum percolation threshold [21].

Our results confirm previous research demonstrating the effect of object shape on the threshold for continuum percolation. We furthermore find that the incorporation of random orientations of objects in continuum percolation simulations significantly affects the percolation threshold. Most of these effects are predicted by the application of excluded volume theory to the calculation of the percolation threshold but, surprisingly, allowing squares to randomly orient decreases  $B_c$  in 2-D whereas random orientation of cubes increases  $B_c$  in 3-D.

### Acknowledgements

We thank P. Bourke, R. Consiglio, L.R. da Silva and S. Havlin for discussions and BP, NSERC, and NSF for support.

---

- [1] D. Ben-Avraham and S. Havlin, *Diffusion and Reactions in Fractals and Disordered Systems* (Cambridge University Press, Cambridge, 2000).
- [2] A. Bunde and S. Havlin, eds., *Fractal and Disordered Systems, Second Edition* (Springer-Verlag, Berlin, 1996), and references therein.
- [3] M. Sahimi, *Applications of Percolation Theory* (Taylor and Francis, London, 1994).
- [4] D. Stauffer and A. Aharony *Introduction to Percolation Theory* (Taylor and Francis, London, 1994).
- [5] E. J. Garboczi, K. A. Snyder, J. F. Douglas, and M. F. Thorpe, Phys. Rev. E, **52**, 819 (1995) .
- [6] U. Alon, A. Drory, and I. Balberg, Phys. Rev. A **42**, 4634 (1990).
- [7] E.T. Gawlinski and H. E. Stanley, J. Phys. A: Math. Gen. **14**, L291 (1981).
- [8] A. Geiger and H.E. Stanley, Phys. Rev. Lett. **49**, 1895 (1982).
- [9] P. L. Leath, Phys. Rev. B **14**, 5046 (1976).
- [10] C. D. Lorenz and R. M. Ziff, J. Chem. Phys. **114**, 3659 (2001).
- [11] Three different sizes of objects were used in the 3-D simulations to confirm the independence of the percolation threshold from both object and system size. Unfortunately our range of system and object size in both 2-D and 3-D simulations is constrained by computer memory restrictions and CPU time available.
- [12] P. Bourke, <http://astronomy.swin.edu.au/pbourke/geometry/lineline2d/>.
- [13] P. Bourke, <http://astronomy.swin.edu.au/pbourke/geometry/linefacet/>.
- [14] H. G. Ballesteros, L. A. Fernandez, V. Martin-Mayor, A. Munoz Sudupe, G. Parisi, and J. J. Ruiz-Lorenzo, J. Phys. A **32**, 1 (1999).
- [15] V.K.S. Shante and S. Kirkpatrick, Adv. Phys. **20**, 325 (1971).
- [16] P. R. King, *North Sea Oil and Gas Reservoirs-II* (The Norwegian Institute of Technology, Graham and Trotman, 1990), Chapter 21, p. 353.
- [17] E. J. Garboczi, M. F. Thorpe, M. S. DeVries and A. R. Day, Phys. Rev. A **43**, 6473 (1991).
- [18] M. A. Dubson and J. C. Garland, Phys. Rev. B **32**, 7621 (1985).
- [19] W. Xia and M. F. Thorpe, Phys. Rev. A **38**, 2650 (1988).
- [20] I. Balberg, C. H. Anderson, S. Alexander, and N. Wagner, Phys. Rev. B **30**, 3933 (1984).
- [21] I. Balberg, Phys. Rev. B **31**, 4053 (1985).
- [22] I. Balberg, Phil. Mag. B **56**, 991 (1987).
- [23] Here  $N_c = \eta_c$  because the object volume equals 1.
- [24] T. Kihara, Rev. Mod. Phys. **25**, 831 (1953).

Object	$V_{ex}$ for unit object	$\phi_c$	$N_c$	$B_c$ (calculated)	$B_c$ (literature)
Discs	4	0.67 [19]	1.1087	4.43	$4.5 \pm 0.1$ [21] 4.7 [6]
Aligned squares	4	$0.6666 \pm 0.0004$	$1.098 \pm 0.001$	$4.39 \pm 0.01$	$4.5 \pm 0.1$ [21] 4.7 [6]
Random squares	4.084	$0.6254 \pm 0.0002$	$0.9819 \pm 0.0006$	$4.01 \pm 0.01$	
Spheres	8	0.289573 [10]	0.341889	2.74	2.79 [6]
Aligned cubes	8	$0.2773 \pm 0.0002$	$0.3248 \pm 0.0003$	$2.59 \pm 0.01$	2.60 [6]
Random cubes	11	$0.2236 \pm 0.0002$	$0.2531 \pm 0.0003$	$2.78 \pm 0.01$	

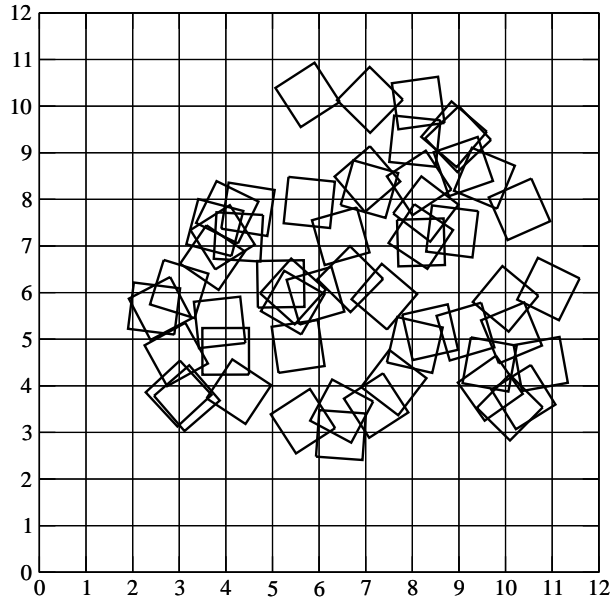


FIG. 1. Two-dimensional,  $12 \times 12$  example of a percolation cluster of unit-length square objects (thick lines) for the case of randomly oriented squares. The system is divided by a series of grid lines (thin lines) that create unit areas in this 2-D system. Note that the upper two objects of the cluster in the center of the system intersect each other even though their centers are placed in next-nearest-neighbor areas of the grid. The real 2-D and 3-D systems of our study are much larger than this system.

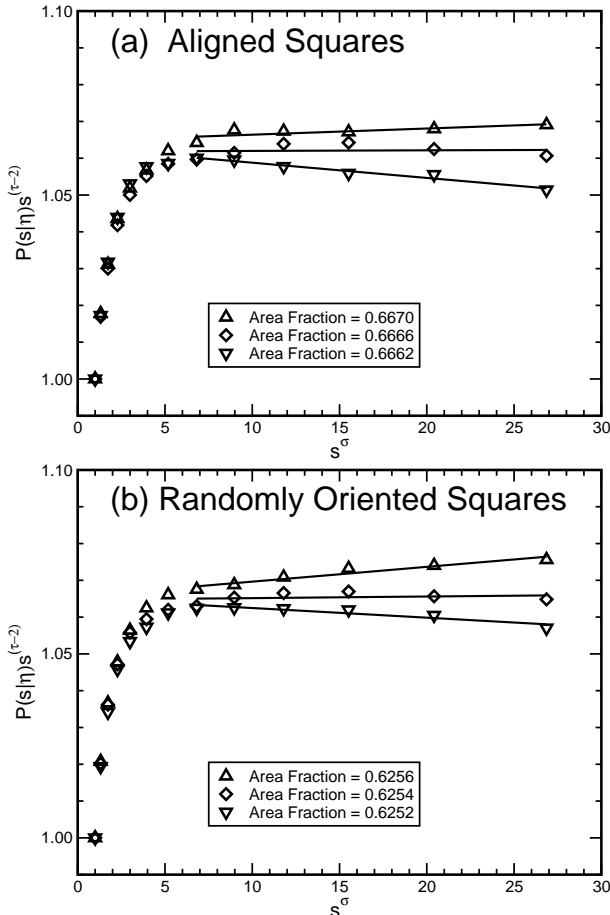


FIG. 2. Power-law scaled plots for determination of percolation threshold for squares of unit size in a  $301 \times 301$  system based upon 50,000 realizations at each area fraction. At the threshold  $\eta = \eta_c$ ,  $P(s|\eta)s^{\tau-2}$  is independent of  $s^\sigma$ , which allows for accurate determination of  $\eta_c$ , which is related to  $\phi_c$  by Eq. 5. (a) Squares whose edges are aligned parallel to each other, for which case we estimate  $\eta_c = 1.098 \pm 0.001$ , so  $\phi_c = 0.6666 \pm 0.0004$  by Eq. 5. (b) Squares that are randomly oriented as shown in Fig. 1, for which we estimate  $\eta_c = 0.9819 \pm 0.0006$ , so  $\phi_c = 0.6254 \pm 0.0002$ .

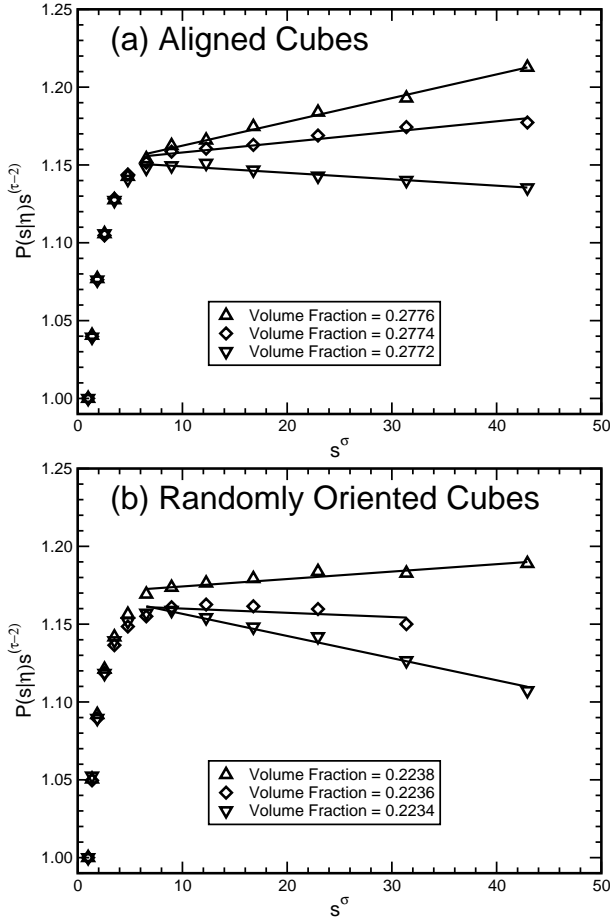


FIG. 3. Power-law scaled plots for determination of percolation threshold for cubes of unit size in a  $161 \times 161 \times 161$  3-D system based upon 50,000 realizations for each volume fraction. At the threshold  $\eta = \eta_c$ ,  $P(s|\eta)s^{\tau-2}$  is independent of  $s^\sigma$ , which allows for accurate determination of  $\eta_c$ , which is related to  $\phi_c$  by Eq. 5. (a) Cubes whose faces are aligned parallel to each other, for which we estimate  $\eta_c = 0.3248 \pm 0.0003$ , so by (5)  $\phi_c = 0.2773 \pm 0.0002$ . (b) Cubes that are randomly oriented, for which we estimate  $\eta_c = 0.2531 \pm 0.0003$ , so  $\phi_c = 0.2236 \pm 0.0002$ .